First principle study of the electronic structure of hafnium-doped anatase TiO_2

Li Lezhong(李乐中)†, Yang Weiqing(杨维清), Ding Yingchun(丁迎春), and Zhu Xinghua(朱兴华)

Department of Optics and Electronics, Chengdu University of Information Technology, Chengdu 610225, China

Abstract: Crystal structures and electronic structures of hafnium doping anatase TiO_2 were calculated by first principles with the plane-wave ultrasoft pseudopotential method based on the density functional theory within the generalized gradient approximation. The calculated results show that the lattice parameters a and c of Hf-doped anatase TiO_2 are larger than those of intrinsic TiO_2 under the same calculated condition. The calculated band structure and density of states show that the conduction band width of Hf-doped TiO_2 is broadened which results in the band gap of Hf-doped being smaller than the band gap of TiO_2.

Key words: Hf-doped; anatase TiO_2; first principle; crystal structure; electronic structure

DOI: 10.1088/1674-4926/33/1/012002 **EEACC:** 2520

1. Introduction

Titanium dioxide (TiO_2) has three commonly encountered polymorphs in nature, which are anatase, rutile and brookite. It was found that the anatase TiO_2 has widespread technological applications in photocatalysts, nanostructured solar cells and spintronic devices[1−5].

The anatase TiO_2 has a fundamental band gap of around 3.2 eV[6], which leads to the low energy conversion efficiency of TiO_2 and only absorbs a small portion of the solar spectrum in the ultraviolet region. Recently, great efforts have been made to modify the band structure of TiO_2 to shift its absorption edge toward the visible light region and place its band edges at proper positions, thus improving its photocatalytic efficiency[5, 7−25]. Doping with transitional metal ions has also been investigated extensively for expanding the photo response of TiO_2 into the visible region[14−25]. For example, Lettmann *et al.* reported that TiO_2 doped with metal ions, such as Ru^{3+}, Rh^{3+}, Pt^{4+} and Ir^{3+}, exhibited visible light activity for the degradation of 4-chlorophenol[20]. Kisch and co-workers also investigated the photocatalytic degradation of 4-chlorophenol under visible irradiation on TiO_2 modified with chloride complexes of Pt, Ir, Rh, Au, Pd, Co and Ni, which is quite different from a typical metal ion-doped titania system[24]. Trenczek-Zajac *et al.* reported that TiO_2 doped with Cr^{3+} ions, exhibited impurity band is formed within the forbidden band gap of titanium dioxide which results in the additional absorption within the visible range of the light spectrum[25].

However, to our knowledge, there are few reports on the study of hafnium-doped TiO_2 either theoretically or experimentally. In this study, the plane-wave-based ultrasoft pseudopotential method based on the density functional theory within the generalized gradient approximation (GGA) has been utilized to investigate the electronic structures of TiO_2 doped by Hf to modify the band structure of TiO_2 to shift its absorption edge toward the visible light region. With the doping of Hf, the band gap becomes narrower than of standard TiO_2.

2. Calculation models and methods

Anatase TiO_2 has a tetragonal structure (space group: $I4_1/amd$, local symmetry: D_{4h}^{19}) and contains four Ti atoms and eight O atoms in the primitive cell. Our model is shown in Fig. 1.

In this work, we have applied the Cambridge serial total energy package (CASTEP) program[26−30] to the structural optimizations of anatase TiO_2 and Hf-doped anatase TiO_2. CASTEP is a first principle quantum mechanical process based on the density function theory (DFT). It uses a total energy plane-wave pseudopotential method. The electronic exchange-correlation energy is treated within the framework of the generalized gradient approximation (GGA). In order to allow calculations to be performed with the lowest possible cut-off energy for the plane-wave basis set, ultrasoft pseudopotentials

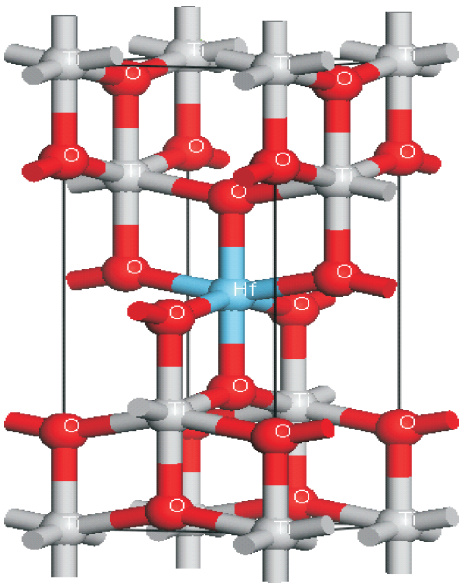

Fig. 1. Unit cell model of Hf-doped anatase TiO_2.

† Corresponding author. Email: lezhongli@cuit.edu.cn
Received 28 May 2011, revised manuscript received 31 August 2011

Table 1. Structural parameters for anatase TiO_2 and Hf-doped TiO_2 compared to the results of experiment.

Parameter	a (Å)	c (Å)	α (°)	γ (°)
TiO_2^{cal}	3.819	9.871	90	90
TiO_2^{exp}*	3.782	9.502	—	—
HTO	3.92	10.21	90	90

*The experimental data is from Ref. [32].

(USPP) have been used in the calculations[31]. Pseudoatomic calculations are performed for Ti $3s^2 3p^6 3d^2 4s^2$, Hf $5d^2 6s^2$ and O $2s^2 2p^4$. In all the high-precision calculations, the cut-off energy of the plane-wave basis set is 350 eV for both TiO_2 and Hf-doped TiO_2. The special points sampling integration over the Brillouin zone are carried out using the Monkhorst–Pack method with a $7 \times 7 \times 3$ special k-point mesh. The total energy is considered to be converged when the self-consistent field (SCF) tolerance is 10^{-6} eV/atom. These parameters are sufficient in leading to well-converged total energy and structural transition calculations.

3. Results and discussion

3.1. Structural properties

The hafnium-doped anatase TiO_2 (HTO) unit cell used in the calculation was generated by replacing one of the titanium atoms with a hafnium atom. The geometric optimization was performed using Broyden–Fletcher–Goldfarb–Shanno (BFGS) minimization algorithm. The equilibrium structure was obtained by minimizing the total energy and forces (the maximal force on each atom is less than 0.03 eV/nm). The final configuration of the anatase TiO_2 and HTO unit cell is shown in Table 1.

From Table 1, we can see that the lattice parameters were overestimated by about 1.0% (a axis) and 3.9% (c axis) compared with the experimental data in Ref. [32]. However, the calculated lattice parameters a and c in our paper are in good agreement with the data of Ref. [33]. The lattice parameters were overestimated, which is attributed to the following two reasons: (1) the inherent problem associated with GGA, which usually overestimates the parameters; (2) the relatively lesser atom numbers (only 12 atoms) of the anatase TiO_2 unit cell for the calculation also brings on the small errors.

As the radius of Hf^{4+} ion (0.79 Å) is larger than that of Ti^{4+} ion (0.68 Å), both the lattice parameters, a and c, of HTO are larger than those of TiO_2 (see Table 1) at the same calculated condition. In this study we have obtained the apical and equatorial O–Hf bond lengths, 1.967 and 2.082 Å, respectively, which are much larger than those of O–Ti, 1.931 and 1.962 Å.

3.2. Band structure and density of states

Figure 2 shows the band structure of TiO_2 along the high symmetry point across the first Brillouin zone. The Fermi level was set as the maximum of the valence band. The corresponding total and partial DOS are shown in Fig. 3. The highest valence band, which is located between –1.916 eV, and the Fermi level, which was formed by the bonding state of the hybridized O2p–Ti3d orbit. The conduction band located between 2.232 and 3.469 eV up the Fermi level which was formed primarily by the Ti3d orbit with minor contribution from O2p orbit. Obviously, the calculated band gap of TiO_2 is 2.232 eV, smaller than the experimental band gap 3.2 eV[6]. It is worth nothing that this calculated band gap is smaller than the experimental result due to the inherent drawback of the ideal electron gas model in GGA approach[1]. From Fig. 2, the conduction band minimum (CBM) is located at G, and the energy of the valence band maximum (VBM) is also located at G. So the anatase TiO_2 can be seen as direct band gap semiconductor[13, 34].

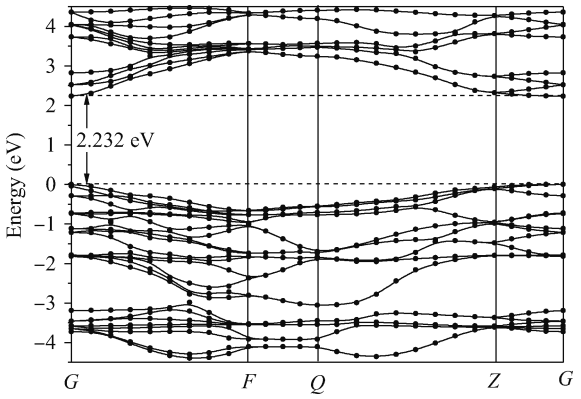

Fig. 2. Band structure of TiO_2.

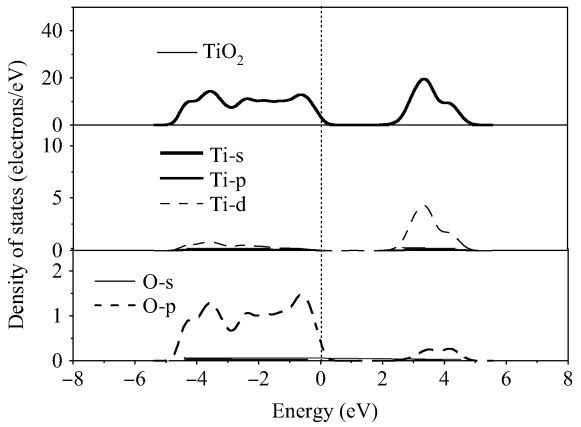

Fig. 3. TDOS and PDOS of TiO_2.

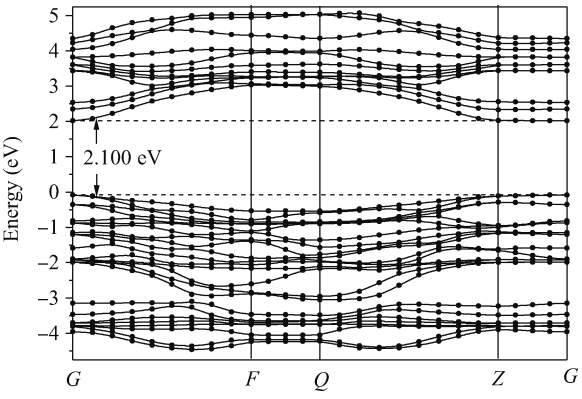

Fig. 4. Band structure of Hf-doped TiO_2.

Figure 4 shows the electronic band structure of Hf-doped TiO_2. The highest valence band was formed by the bonding

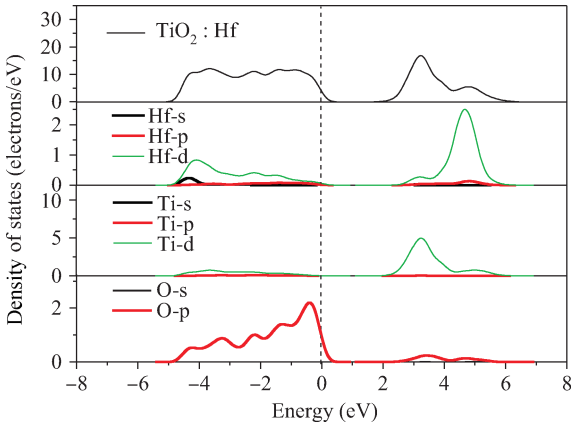

Fig. 5. TDOS and PDOS of Hf-doped TiO_2.

state of the hybridized O2p–Ti3d–Hf5d orbit. The conduction band up the Fermi level was formed primarily by the Ti3d and Hf5d orbits with minor contribution from O2p orbit. The calculated band gap of the Hf-doped TiO_2 is 2.100 eV, which is 0.132 eV less than that of the intrinsic TiO_2. The narrower band gap of Hf-doped TiO_2 indicates that the absorption edge redshifts toward visible-light region. Unfortunately, so far, no related experimental data are yet available for a comparison with this theoretical result.

For further analyzing the constitution of VB and CB, and understanding the change of electronic structures brought by Hf-doped TiO_2, the calculated total density of states (TDOS) and partial density of states (PDOS) are shown in Fig. 5. It is clear that the VB of Hf-doped TiO_2 is formed mainly by the O2p states and Ti3p states, the CB consists mainly of Ti3d states, and the CB is formed by hybridization of Ti3d states with Hf5d states. The CB width (1.77 to 5.23 eV) of TiO_2 is 3.46 eV, and the CB width (1.60 to 6.51 eV) of Hf-doped TiO_2 is 4.91 eV. Compared with that of TiO_2, we can see the CB width of Hf-doped TiO_2 is broadened, and the CBM shift much downward 0.17 eV. For the VBM of TiO_2 and Hf-doped TiO_2, one is located at 0.53 eV, the other is at 0.56 eV, and the VBM of Hf-doped shift much downward 0.03 eV. As a result, the band gap of Hf-doped TiO_2 is 0.132 eV less than the band gap of TiO_2.

4. Conclusions

The TiO_2 crystal, electronic structures of TiO_2 and hafnium-doped TiO_2 were calculated using the first principle method. The calculation on Hf-doped TiO_2 with GGA shows that the lattice parameters are larger than TiO_2 both a and c, and the CB width of Hf-doped TiO_2 is broadened which results in the band gap of Hf-doped being 0.132 eV less than the band gap of TiO_2.

References

[1] Fujishima A, Honda K. Electrochemical photocatalysis of water at a semiconductor electrode. Nature, 1972, 37: 238
[2] Grazel M. Photoelectrochemical cells. Nature, 2001, 414: 338
[3] Khan S, Al-Shahry J M, Ingler W B. Efficient photochemical water splitting by a chemically modified n-TiO_2. Science, 2002, 297: 2243
[4] Hoffmann M R, Martin S T, Choi W Y, et al. Environmental applications of semiconductor photocatalysis. Chem Rev, 1995, 95: 69
[5] Gai Y, Li J, Li S S. Design of narrow-gap TiO_2: a passivated codoping approach for enhanced photoelectrochemical activity. Phys Rev Lett, 2009, 102: 036402
[6] Heller A. Chemistry and applications of photocatalytic oxidation of thin organic films. Accounts of Chemical Research, 1995, 28: 503
[7] Wang Y, Doren D J. First-principles calculations on TiO_2 doped by N, Nd, and vacancy. Solid State Commun, 2005, 136: 186
[8] Asahi R, Morikawa T, Ohwaki T, et al. Visible-light photocatalysis in nitrogen-doped titanium oxides. Science, 2001, 293: 269
[9] Torres G R, Lindgren T, Lu J. Photoelectrochemical study of nitrogen-doped titanium dioxide for water oxidation. J Phys Chem B, 2004, 108: 5995
[10] Umebayashi T, Yamaki T, Itoh H, et al. Band gap narrowing of titanium dioxide by sulfur doping. Appl Phys Lett, 2002, 81: 454
[11] Gole J L, Stout J D, Burda C, et al. Highly efficient formation of visible light tunable $TiO_{2-x}N_x$ photocatalysts and their transformation at the nanoscale. J Phys Chem B, 2004, 108: 1230
[12] Irie H, Watanabe Y, Hashimoto K. Carbon-doped anatase TiO_2 powders as a visible-light sensitive photocatalyst. Chem Lett, 2003, 32: 772
[13] Gao Pan, Zhang Xuejun, Zhou Wenfang, et al. First-principle study on anatase TiO_2 codoped with nitrogen and ytterbium. Journal of Semiconductors, 2010, 31: 032001
[14] Ohno T, Tanigawa F, Fujihara K, et al. Photocatalytic oxidation of water by visible light using ruthenium-doped titanium dioxide powder. Journal of Photochemistry and Photobiology A: Chemistry, 1999, 127: 107
[15] Zhao G, Kozuka H, Lin H, et al. Sol–gel preparation of $Ti_{1-x}V_xO_2$ solid solution film electrodes with conspicuous photoresponse in the visible region. Thin Solid Films, 1999, 339: 123
[16] Klosek S, Raftery D. Visible light driven V-doped TiO_2 photocatalyst and its photooxidation of ethanol. J Phys Chem B, 2001, 105: 2815
[17] Li X Z, Li F B. Study of Au/Au^{3+}–TiO_2 photocatalysts toward visible photooxidation for water and wastewater treatment. Environmental Science and Technology, 2001, 35: 2381
[18] Fuerte A, Hernandez-Alonso M D, Maira A J, et al. Visible light-activated nanosized doped-TiO_2 photocatalysts. Chem Commun, 2001, 24: 2718
[19] Xie Y, Yuan C. CW photocatalysis of neodymium ion modified TiO_2 sol under visible light irradiation. Appl Surf Sci, 2004, 221: 17
[20] Lettmann C, Hinrichs H, Maier W F. Combinatorial discovery of new photocatalysts for water purification with visible light. Angewandte Chemie International Edition, 2001, 40: 3160
[21] Burgeth G, Kisch H. Photocatalytic and photoelectrochemical properties of titania–chloroplatinate (IV). Coordination Chemistry Reviews, 2002, 230: 41
[22] Macyk W, Kisch H. Photosensitization of crystalline and amorphous titanium dioxide by platinum (IV) chloride surface complexes. Chemistry A European Journal, 2001, 7: 1862
[23] Zang L, Macyk W, Lange C, et al. Visible-light detoxification and charge generation by transition metal chloride modified titania. Chemistry A European Journal, 2000, 6: 379
[24] Kisch H, Zang L, Lange C, et al. Modified, amorphous titania—a hybrid semiconductor for detoxification and current generation by visible light. Angewandte Chemie International Edition, 1998, 37: 3034
[25] Trenczek-Zajac A, Radecka M, Jasinski M, et al. Influence of Cr on structural and optical properties of TiO_2:Cr nanopowders pre-

pared by flame spray synthesis. Journal of Power Sources, 2009, 194(1): 104

[26] Clark S J, Segall M D, Pickard C J, et al. First principles methods using CASTEP. Zeitschrift fur Kristallograhie, 2005, 220: 567

[27] Segall M D, Lindan P J D, Probert M J, et al. First-principles simulation: ideas, illustrations and the CASTEP code. Journal of Physics: Condensed Matter, 2002, 14: 2717

[28] Sun J, Wang H J, He J L, et al. Ab initio investigations of optical properties of the high-pressure phases of ZnO. Phys Rev B, 2005, 71: 125132

[29] Hu C H, Wang Y M, Chen D M, et al. First-principles calculations of structural, electronic, and thermodynamic properties of Na_2BeH_4. Phys Rev B, 2007, 76: 144104

[30] StojiN, Corso A D, Zhou B, et al. *Ab initio* simulation of photoemission spectroscopy in solids: plane-wave pseudopotential approach, with applications to normal-emission spectra of Cu(001) and Cu(111). Phys Rev B, 2008, 77: 195116

[31] Vanderbilt D. Soft self-consistent pseudopotentials in a generalized eigenvalue formalism. Phys Rev B, 1990, 41: 7892

[32] Burdett J K, Hughbanks T, Miller G J, et al. Structural-electronic relationships in inorganic solids: powder neutron diffraction studies of the rutile and anatase polymorphs of titanium dioxide at 15 and 295 K. Journal of the American Chemical Society, 1987, 109: 3639

[33] Muscat J, Swamy V, Harrison N M. First-principles calculations of the phase stability of TiO_2. Phys Rev B, 2002, 65: 224112

[34] Minoura H, Nasu M, Takahashi Y. Comparative studies of photoelectrochemical behavior of rutile and anatase electrodes prepared by OMCVD technique. Berichte der Bunsen-Gesellschaft, 1985, 89(10): 1064